ISSN 0003-6838, Applied Biochemistry and Microbiology, 2023, Vol. 59, No. 3, pp. 297–307. © Pleiades Publishing, Inc., 2023.

Isolation and Identification of a Novel Cellulolytic and Glucose-tolerant *Trichoderma* Isolate from Forest Soils in Iran

S. Dehghan[a], M. Seyedabadi[a], A. Mirshamsi Kakhki[a, *], M. Farsi[a], and A. Seifi[a]

[a] *Department of Biotechnology and Plant Breeding, Faculty of Agriculture, Ferdowsi University of Mashhad, Mashhad, 9177948974 Iran*

**e-mail: mirshamsi@um.ac.ir*

Received August 6, 2022; revised December 22, 2022; accepted January 9, 2023

Abstract—*Trichoderma* species are known to have a high potential for biotechnological applications. β-glucosidase enzyme is an important component of cellulase enzyme complex of *Trichoderma* with a crucial role in enzymatic degradation which is inhibited by glucose. The purpose of this study was to find the *Trichoderma* strains with high cellulase activity and tolerance to glucose. Therefore, 77 *Trichoderma* isolates were obtained from forest soils in Iran. Ten of them, had high cellulase activity, and the H1N44 isolate showed the highest activity of cellulase as well as high tolerance to glucose. In addition using FPAse assay, the level of cellulase activity was 0.66 U/mL in H1N44 and this result was 4-fold higher than β-glucosidase activity in *Trichoderma reesei* QM6a in the absence of glucose. Then, 10 representative cellulolytic isolates were sequenced in three genomic loci, including ITS, *tef-1* and *rpb-2* and H1N44 isolate was recognized as *Trichoderma koningiopsis*. As a result of this study, H1N44 was identified as a novel cellulolytic and glucose-tolerant strain with high potential for biotechnological utilization.

Keywords: *Trichoderma*, cellulase, β-glucosidase, glucose, ITS, *tef-1*, *rpb-2*

DOI: 10.1134/S0003683823030067

Lignocellulosic biomass is an abundant renewable organic resource in nature and a potential alternative for fossil fuels. By hydrolyzing biomass to fermentable sugars with fungal enzymes, it can be converted into ethanol and via biorefinery to other platform chemicals for the sustainable bio-economy. Cellulases and hemicellulases are 2 large families of enzymes which are capable of hydrolyzing lignocellulose to monomeric sugars [1, 2]. Cellulases are one of the most important industrial enzymes and have an enormous potential for applications in different industries such as juice extraction, detergent enzymes, textile, paper, food and animal feed industries, bioenergy and biofuels [3].

Due to the efficient degradation of plant biomass, the filamentous fungus *Trichoderma reesei* is one of the most widely used platform microorganisms in the industry as a source of cellulases and hemicellulases The *Trichoderma* cellulase system consists of exoglucanase (EC.3.2.1.91), endoglucanase (EC.3.2.1.4) and β-glucosidases (BGL) (EC.3.2.1.21) that synergistically degrade cellulose. BGLs complete cellulose hydrolysis by converting cellobiose to glucose (Glu). It has been reported that the BGL activity in *T. reesei* is lower than the other two enzymes and is also highly sensitive to high Glu concentrations. Both of these deficiencies cause the accumulation of cellobiose in the medium which acts as an inhibitor for exoglucanase and endoglucanase. Therefore, the optimal secretion of BGLs as well as the Glu tolerance is closely linked to the economical production of bioethanol [2].

There are several alternative approaches to enhance BGL activity such as co-cultivation of some cellulolytic fungi with high BGL activity, heterologous expression of some BGLs, use of promoter to enhance the activity and site-directed mutagenesis [4–6]. Because of the ability of BGLs to hydrolyze and synthesize glycosidic bonds also wide variety of substrates, they have many applications in industry [7] such as improving the aroma of fruit juice and wine, hydrolyzing soybean isoflavone glycosides, reducing the toxicity of animal feed, producing anti-cancer compounds, and degrading cellulose to convert lignocellulosic biomass in biofuel production. Glu-tolerant BGLs can help improve many processes. For example, 0.8 unit of BGL with Ki of 4.28 M for Glu could completely hydrolyzed soybean isoflavone glycosides. Another example is the use of glucose-tolerant BGL in wine processing that could release aromatic-related compounds while keep the activity at low pH as well as 10–20% Glu [7]. The use of Glu-tolerant BGL has also been considered in production of biofuels because of increasing the efficiency of the process. Regarding these applications of BGLs, fungi containing Glu-tolerant BGLs are expected in nature. Therefore, isola-

Table 1. Origin of *Trichoderma* isolates and depth of sampling

Name of isolate	Forest area	Depth, cm
A2N2, A2N17	Shahid Bahonar Park, Kerman	5–10
C2N9	Sirch, Kerman	5–10
D1N1, D1N2, D1N3, D1N5	Walnut Forest, Sirch, Kerman	0–5
D2N3	Walnut Forest, Sirch, Kerman	5–10
E1N16, E1N17, E1N19	Halimeh Jan, Rudbar, Gilan	0–5
F1N1, F1N2, F1N3, F1N5, F1N11	Lakan, Rasht, Gilan	0–5
F2N1, F2N4, F2N7, F2N8	Lakan, Rasht, Gilan	5–10
G1N5	Namak Abrud Park, Chalus, Mazandaran	0–5
G2N1, G2N2, G2N3	Namak Abrud Park, Chalus, Mazandaran	5–10
H1N1, H1N2, H1N3, H1N12, H1N16, H1N17, H1N18, H1N19, H1N20, H1N21, H1N22, H1N23, H1N24, H1N26, H1N27, H1N28, H1N29, H1N31, H1N36, H1N39, H1N40, H1N43, H1N44, H1N45, H1N46, H1N47	Chalus, Mazandaran	5–10
H2N2, H2N5, H2N6	Chalus, Mazandaran	5–10
I1N13	Marzan Abad, Chalus, Mazandaran	0–5
I2N18, I2N26, I2N27, I2N28, I2N30	Marzan Abad, Chalus, Mazandaran	5–10
K1N2, K1N3, K1N5, K1N6, K1N9, K1N10, K1N20, K1N21, K1N26, K1N27, K1N29,	Si Sangan Forest Park, Nowshahr, Mazandaran	0–5
K2N13, K2TN1	Si Sangan Forest Park, Nowshahr, Mazandaran	5–10
M1N2, M1N7, M1N8, M1N12	Saravan Park, Rasht, Gilan	0–5
M2N9	Saravan Park, Rasht, Gilan	5–10

tion of such fungi can help to design efficient enzyme cocktails for the degradation of plant biomass [2].

Trichoderma species can be found in a wide range of ecosystems, in several types of soil (like forest soils, salt marshes, agricultural lands and even soils of deserts), various plant parts and woods, and in the water [8]. Gams and Bissett [9] described some distinctive characteristics for morphological identification of *Trichoderma* species at the genus level. Although morphological analysis has been a common method for identification of *Trichoderma* species, it can lead to incorrect identification at the species level due to the morphological similarity between close species and the need for special expertise. Therefore, it is necessary to validate the initial observations by molecular methods [10, 11]. Some informative loci of the translation elongation factor ef-1-α (*tef-1*), RNA polymerase II subunit B2 (*rpb-2*), chitinase 18-5 (*ech-42*), calmodulin 1 (*calm-1*), actin, β-tubulin 2 (*tub-B2*), nuclear protein (*las-1*) and subunit A of ATP citrate lyase (*aclA*), should be included for identification studies [12].

In the current work, 77 *Trichoderma* strains were isolated from forest soils in Iran and 10 isolates were selected for sequencing in 3 gene loci which were chosen based on the cellulase activity resulted from Congo red test. The objective of this study was to find the best cellulolytic isolate. To this end, the isolates were screened qualitatively and quantitatively for cellulase and BGL activity. Our findings showed that the cellulolytic strain H1N44 can be used for further studies and would be promising strain in biotechnological applications in future because of its high BGL activity and low Glu inhibition.

MATERIALS AND METHODS

Isolation of fungi from soil. Soil samples were collected from 7 forest areas in the north and 4 areas in the southeast of Iran for isolation of cellulolytic fungi (Table 1). Sampling was performed at two soil depths (0–5 and 5–10 cm) from 3 different locations in each area. These samples were mixed as a representative sample from each location. Then samples were transferred to the laboratory to be stored at 4°C.

Serial dilution method was used for isolation of *Trichoderma* isolates from soil. First, the 10 g soil samples were weighed into bags, and then each sample was added to tubes containing 90 mL of distilled sterile water and shaken for 30 min at 260 rpm for homogenization. Serial dilution was performed up to 10^{-6}. Then 200 μL from each dilution was inoculated onto RBG medium containing (g/L): peptone—5.0, Rose Bengal—0.05, Glu—10.0, dipotassium phosphate—1.0,

$MgSO_4 \cdot 7\ H_2O$—0.5 and agar—15.0. After autoclaving, the medium was supplemented with chloramphenicol (0.1 g/L). All the plates were incubated at 28°C for 2–4 days and growth was observed daily.

After 2–4 days, single clones were transferred into water agar medium. The water agar medium is a nutrition-deprived medium that helps to spread fungal hypha in the plate. Then single hypha was isolated under a binocular and transferred to PDA medium containing (g/L): potato—4.0, dextrose—20.0, agar—18.0. These plates were incubated at 28°C for 5–8 days. Further purification was done for some impure cultures by subculturing from original PDA plates to new separated plates and repeated several times to reach pure cultures using for morphological identification.

Morphological identification. *Trichoderma* isolates were initially classified based on macroscopic features such as colony color and reverse color, shape of colony, growth pattern and growth rate. Then, all likely *Trichoderma* fungi were analyzed under a light microscope (Olympus DP20 microscopic camera, Olympus, Japan). Staining was performed by lactophenol cotton blue staining. A small portion of mycelia of 3–5 days-old fungi was taken by a sterile needle and put in a drop of lactophenol cotton blue on a microscopic slide. After the mycelia were immersed in the dye, a coverslip was placed on the slide and microscopic features such as conidiophore characters, branching, phialid characters, phialid arrangement, shape and color of conidia were observed (100× magnification) and recorded under the microscope. Size of conidia, phialids and conidiophores were measured with the ImageJ software 1.52a.

Primary screening for cellulase activity. Congo red test was used for selection of isolates with desirable cellulase activity [13]. For this purpose, the growth medium contained (g/L): $NaNO_3$—3.0, K_2HPO_4—1.0, $MgSO_4$—0.5, KCl—0.5, agar—20.0 and carboxymethyl cellulose (CMC)—10.0 (as a sole carbon source) supplemented with 0.01 mg/L $FeSO_4 \cdot 7H_2O$. The pH was adjusted to 5.0 prior to sterilization. The plates with mycelial isolates were incubated at 30°C for 96 h, then at 45°C for 18 h and growth of fungi was measured by diameter of the colony. Ten mL 0.2% Congo red was added to the plates, discarded after 15 min, then the plates were washed with 10 mL 1M NaCl. The clear zone was observed around the colony and diameter of this halo was measured, thereby the enzymatic index (EI) was calculated using the following equation:

$$EI = \frac{\text{diameter of halo}}{\text{diameter of colony}}.$$

Molecular identification. ITS, *tef-1 and rpb-2* PCR amplification. DNA extraction was carried out from mycelia of 5 days-old cultures [14] of 10 *Trichoderma* isolates selected based on the Congo red test. ITS-PCR, *tef-1*-PCR and *rpb-2*-PCR were done in these selected isolates, purified and sent to the Eurofins Genomics Company for sequencing.

The ITS regions including ITS-1, 5.8S rRNA, ITS-2, fragment of the large intron of the *tef-1* gene encoding translation elongation factor 1-α, and RNA polymerase II subunit B gene (*rpb-2*) fragment, were amplified by PCR using the universal primers ITS1 (5'-TCCGTAGGTGAACCTGCGG-3') and ITS4 (5'-TCCTCCGCTTATTGATATGC-3') for ITS regions, the primer pair EF1-728F (5'-CATCGAGAAGTTCGAGAAGG-3') and EF1-986R (5'-TACTTGAAGGAACCCTTACC-3') for *tef-1* fragment and the primer pair fRPB2-5f (5'-GAYGAYMGWGATCAYTTYGG-3') and fRPB2-7cr (5'-CCCATRGCTTGTYYRCCCAT-3') for the *rpb-2* fragment. PCR reactions were done using 50–100 ng of genomic DNA as a template, 0.5 μM of each primer, 0.2 mM of dNTPs, 1X Phusion HF buffer, and 1 unit Phusion DNA polymerase in a total volume of 50 μL. PCR program was consisted of an initial denaturation step of 98°C for 30 s, then 35 cycles of denaturation at 94°C for 10 s, primer annealing at 54°C for ITS-PCR, 56°C for *tef-1*-PCR and 53°C for *rpb-2*-PCR for 30 s and elongation at 72°C for 30 s and final elongation step at 72°C for 10 min. The phylogenetic trees were drawn using MEGA 5.2 and the maximum likelihood method based on Kimura-2 parameters with 1000 bootstrap replications.

Enzyme production. Erlenmeyer flasks (250 mL) were used for enzyme production. The cultures were grown in modified Mandels medium containing (g/L): KH_2PO_4—2.0, $(NH_4)_2SO_4$—1.4, urea—0.3, $MgSO_4 \cdot 7H_2O$—0.3, $CaCl_2 \cdot 2H_2O$—0.4, lactose—0.8 and wheat bran 5.0 (a carbon source) supplemented with (mg/L): $FeSO_4 \cdot 7H_2O$—5.0, $MnSO_4 \cdot 7H_2O$— 1.56, $ZnSO_4 \cdot 7H_2O$—1.4 and $CoCl_2 \cdot 6H_2O$—3.67 [15]. The pH was adjusted to 5.0 prior before sterilization. The flasks containing 50 mL of this medium were inoculated by 5 mL conidial suspension (10^7 conidia/mL) and incubated at 30°C and 200 rpm for 7 days. After this period, the culture supernatant was collected by centrifugation (1500 *g* for 5 min at 4°C) and used as the enzyme source.

Enzyme assays. Total cellulase activity (filter paper assay; FPA) was measured according to the method described by Ghose [16]. According to this, 0.5 mL of the enzyme solution with 1 mL 50 mM citrate buffer (pH 4.8) containing 50 mg filter paper (Whatman no.1, UK) were incubated at 50°C for 60 min. After reaction with DNS reagent, the OD_{540} was measured.

BGL activity was measured within a 3 ml volume, containing 5 mM p-nitrophenyl β-D-glucopyranoside (pNPG), 100 mM acetate buffer (pH 4.0) and suitable amount of enzyme. After the solution being incubated for 30 min at 50°C, the reaction was stopped by adding 1 M sodium carbonate. Thereafter, the absorption of released *p*-nitrophenol (pNP) was measured at 430 nm [17]. BGL activity was also measured

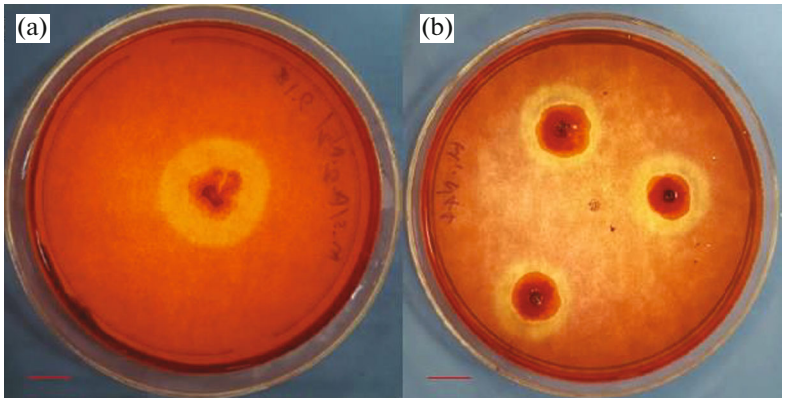

Fig. 1. The clear zone caused by hydrolyzing the CMC using Congo red dye staining. (a) H1N44 isolate in initial screening which showed the best cellulase activity with EI of 2.6. (b) H1N44 isolate in the presence of 25% wt/vol Glu (secondary screening) with EI of 1.6 indicating the best tolerance to Glu among the most highly cellulolytic and Glu-tolerant isolates.

at different concentrations of Glu, temperatures and pH: (0.2, 0.4, 0.6, 0.8, 1 M), (30, 40, 60, 70, 80°C), (pH of 5.6, 5.0, 4.8, 4.4, 4.0, and 3.6), respectively.

Protein quantification was carried out according to the Bradford method [18] using BSA as a standard.

Isolation of *bgl2* gene encoding BGLII enzyme. The available coding sequences of *bgl2* orthologues in *Trichoderma* strains (such as *T. reesei, T. virens, T. harzianum, T. longibrachiatum, T. asperellum*) were used to design the primer pairs for isolation of *bgl2* sequence in the selective isolate, H1N44. The primer pairs (F: 5'-ATGTTGCCCAAGGACTTTCAGTG) (R: 5'-CTCTTTGCGCTCTTCTTSGG) were designed based on the conserved sequences in these 5 strains and used for amplifying a partial sequence of *bgl2* gene.

RESULTS AND DISCUSSION

Morphological and microscopic features of *Trichoderma* isolates. About 700 isolates were initially obtained and grown on PDA plates for identification based on morphological features. Based on the description given by identification keys for fungi, nearly 100 candidate strains that were likely to be *Trichoderma* were selected. Further confirmation was done by microscopic analysis, and finally 77 isolates were identified as being likely from the genus *Trichoderma*.

Soil horizons that are covered with wood, leaves, and rotten branches are considered to be favorable niches for plant cell wall-degrading fungi such as *Trichoderma* due to their role in plant biomass decomposition. Nevertheless, these fungi can also be found in deeper horizons in the soil like in the rhizosphere, where *Trichoderma* species are known to exist as biocontrol fungi with mycotrophic activities against plant pathogens [19].

Out of the 77 identified *Trichoderma* isolates, 22 (29%) were obtained from the top level of soil (0–5 cm of depth) and 55 (71%) from the deeper depth (5–10 cm), indicating that the deeper depth is richer in *Trichoderma* strains. The vast majority of isolates were obtained from the northern forests (69) except for 8 isolates that were from the forest areas in the southeast.

Qualitative screening of *Trichoderma* isolates for cellulolytic activity. The goal of this study was to obtain an isolate with favorable cellulase activity as well as glucose tolerance. In order to this, all 77 isolates were qualitatively compared using plate diffusion tests with Congo red staining in 2 series of screenings. The initial screening revealed that 32 isolates (41%) had a favorable cellulase activity with EI > 1.5, 27% displayed an EI between 1–1.5 and 33% had an EI equal to 1. The isolate H1N44, identified above as a putative strain, was selected as the best isolate with an EI of 2.6.

Due to the inhibitory role of glucose for the BGL, a secondary screening was performed using the 32 strains with an EI > 1.5 on plates supplemented with 25% wt/vol glucose (no halos were observed at higher concentrations; data is not shown) for selection of the most tolerant isolate. Again, the H1N44 isolate (EI of 1.6) was identified among the most highly glucose-tolerant isolates (Fig. 1) together with the isolate I2N27 (EI > 1.5). 16 isolates showed an EI of between 1–1.5 and the others had an EI equal to 1.

Molecular identification of cellulolytic isolates. Out of all 77 isolates, 10 strains showed better cellulase activity than the other isolates based on the Congo red test, were selected for sequencing. The ITS region, a fragment of the large intron of the *tef-1* gene and fragments of RNA polymerase II subunit B gene *rpb-2* were used for the identification of the 10 selected *Trichoderma* isolates at the species level. The sequence size of PCR products was approximately 600, 300, and 1100 bp for ITS, *tef-1*, and *rpb-2* amplicons, respec-

Table 2. Identity of isolated *Trichoderma* strains based on the ITS, *tef-1* and *rpb-2* sequencing using BLASTN and *TrichOKEY* programs (for ITS sequencing)

Isolate name	Recognized strain	Identity (%); e-value; accession number		
		ITS	*tef-1*	*rpb-2*
H1N3	*T. atrobrunneum*	99.47; 0; NR_137298	100; 9e-157; AF443943	100; 0; KX632572
I2N27	*T. harzianum*	100; 0; MN585667	99.3; 8e-152; MT739407	98.82; 0; MT118249
K1N6	*T. harzianum*	100; 0; MW386719	98.99; 2e-149; KX912203	98.62; 0; MG873465
F2N1	*T. orientale*	99.46; 0; NR_111317	99.03; 2e-128; HG931217	100; 3e-151; JQ685884
F1N3	*T. koningiopsis*	99.8; 0; NR_131281	98.74; 1e-156; MF185947	98.85; 2e-125; KT278917
H1N16	*T. koningiopsis*	99.8; 0; NR_131281	99.35; 6e-159; MF185947	98.82; 0; KT278917
H1N44	*T. koningiopsis*	99.8; 0; NR_131281	99.02; 3e-156; MF185947	100; 0; KT278918
M1N12	*T. koningiopsis*	99.8; 0; NR_131281	99.02; 4e-155; MF185947	100; 0; KT278918
F1N1	*T. koningii*	100; 0; NR_138456	98.65; 2e-154; AM498581	100; 0; FJ760541.2
F1N2	*T. koningii*	100; 0; NR_138456	99.31; 1e-147; AM498581	100; 0; FJ760541.2

Table 3. The accession numbers of the sequences generated in this study

Accession numbers for ITS sequences
F1N1 (MZ707734), F1N2 (MZ707735), F1N3 (MZ707736), H1N16 (MZ707737), H1N44 (MZ707738), M1N12 (MZ707739), H1N3 (MZ707740), K1N6 (MZ707741), I2N27 (MZ707742), D2N3 (MZ707743), H1N20 (MZ707744), H1N40 (MZ707745), F2N1 (MZ707746) and H2N2 (MZ707747)
Accession numbers for *tef-1* sequences
F1N1 (OK087563), F1N2 (OK087564), F1N3 (OK087565), H1N16 (OK087566), H1N44 (OK087567), M1N12 (OK087568), H1N3 (OK087569), I2N27 (OK087570), K1N6 (OK087571), F2N1 (OK087572), D2N3 (OK087573), H2N2 (OK087574), H1N20 (OK087575) and H1N40 (OK087576)
Accession numbers for *rpb*-2 sequences
D2N3 (OK087577), F1N1 (OK087578), F1N2 (OK087579), F1N3 (OK087580), H1N16 (OK087581), H1N44 (OK087582), M1N12 (OK087583), F2N1 (OK087584), H1N3 (OK087585), I2N27 (OK087586), K1N6 (OK087587), H1N20 (OK087588), H1N40 (OK087589) and H2N2 (OK087590)
Accession number for *bgl2* sequence
strain H1N44 (OK087591)

tively. All 10 ITS, *tef-1*, and *rpb-2* sequences were analyzed by the BLASTN and *TrichOKEY* programs (https://blast.ncbi.nlm.nih.gov/Blast.cgi; www.isth.info/tools/molkey/). According to this results, the 10 isolates represented 5 species (Table 2).

Sequencing of 10 isolates were identified as being derived from 5 species of *Trichoderma*: *T. atrobrunneum, T. koningii, T. koningiopsis, T. harzianum* and *T. orientale* (Table 3).

The isolate F2N1 was unclear based on the ITS sequencing results and could have represented *T. orientale*, *T. longibrachiatum* or *T. reesei*, while the *tef-1* and *rpb-2* sequences indicated *T. orientale* or *T. longibrachiatum*. According to the phylogeny (Fig. 2), the isolate clustered close to the *T. orientale* reference and clearly separates from *T. longibrachiatum* and *T. reesei* in the trees based on the ITS sequencing results. It was in line with the observed morphological features, including aerial mycelium uniformly cottony on PDA, conidial production forming broad concentric rings, light greenish gray to dark greenish gray, no distinctive odor, and diffusing pale yellow to olive yellow pigmentation [20]. *tef-1* and *rpb-2* sequencing results confirmed that this strain should be *T. orientale*.

Considering isolate H1N3, sequencing provided ambiguous results between the ITS-region and *rpb-2* as well as *tef-1*. The ITS sequencing results indicated that H1N3 is a *T. harzianum* isolate, but *tef-1* and *rpb-2* sequencing results rather suggested that it is likely to be *T. atrobrunneum*, which also aligned better with the grouping suggested by the phylogenetic analysis. These observations can be explained by the fact that the *T. harzianum* species complex includes *T. atrobrunneum* (besides *T. afarasin, T. afroharzianum, T. camerunense, T. endophyticum, T. neotropicale, T. pyramidale, T. rifaii, and T. simmonsii* [21]. Haou-

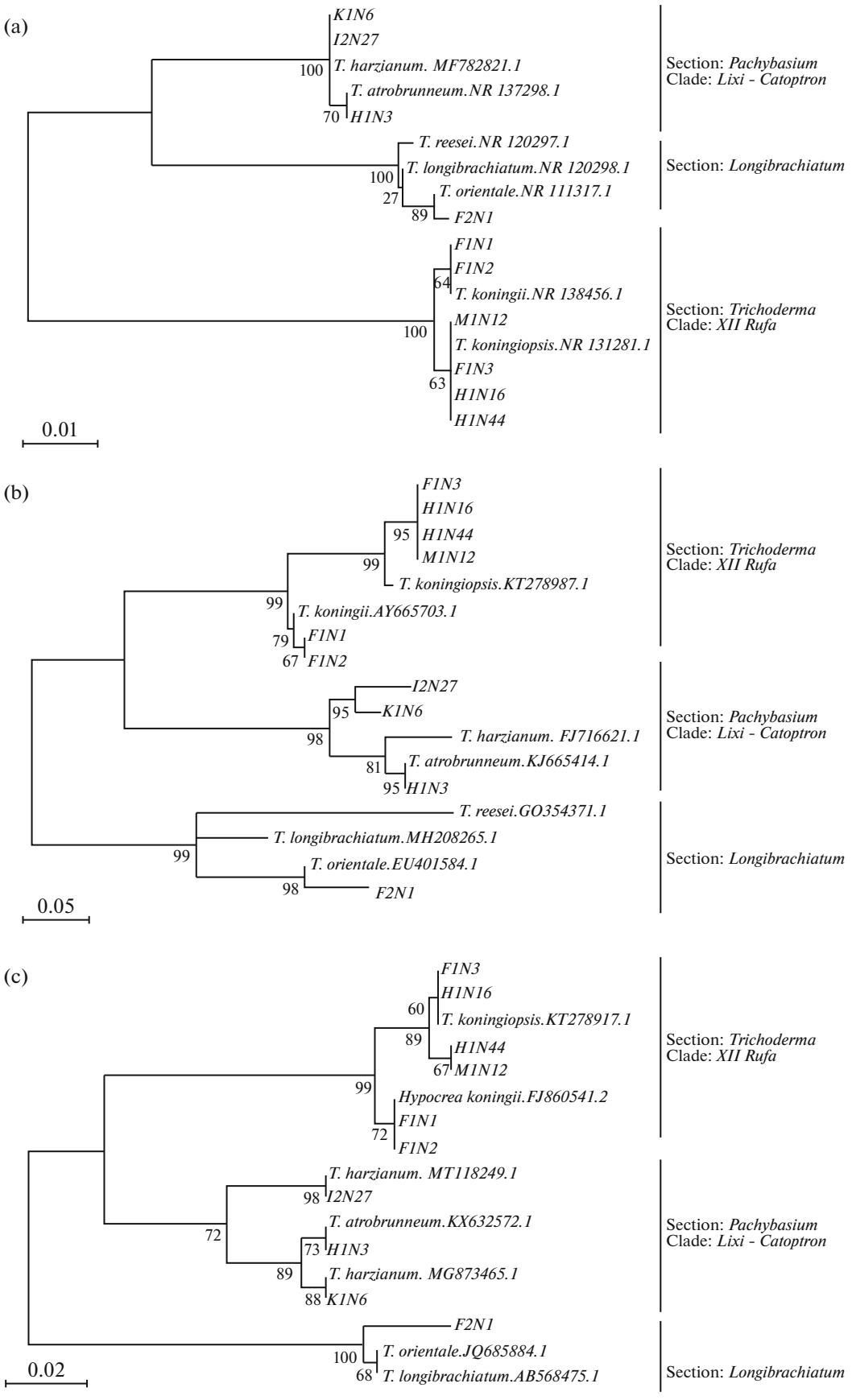
(a)
K1N6
I2N27
T. harzianum. MF782821.1
T. atrobrunneum.NR 137298.1
H1N3
T. reesei.NR 120297.1
T. longibrachiatum.NR 120298.1
T. orientale.NR 111317.1
F2N1
F1N1
F1N2
T. koningii.NR 138456.1
M1N12
T. koningiopsis.NR 131281.1
F1N3
H1N16
H1N44
100
70
100
27
89
64
100
63
0.01
Section: Pachybasium
Clade: Lixi - Catoptron
Section: Longibrachiatum
Section: Trichoderma
Clade: XII Rufa
(b)
F1N3
H1N16
H1N44
M1N12
T. koningiopsis.KT278987.1
T. koningii.AY665703.1
F1N1
F1N2
I2N27
K1N6
T. harzianum. FJ716621.1
T. atrobrunneum.KJ665414.1
H1N3
T. reesei.GO354371.1
T. longibrachiatum.MH208265.1
T. orientale.EU401584.1
F2N1
95
99
99
79
67
95
98
81
95
99
98
0.05
Section: Trichoderma
Clade: XII Rufa
Section: Pachybasium
Clade: Lixi - Catoptron
Section: Longibrachiatum
(c)
F1N3
H1N16
T. koningiopsis.KT278917.1
H1N44
M1N12
Hypocrea koningii.FJ860541.2
F1N1
F1N2
T. harzianum. MT118249.1
I2N27
T. atrobrunneum.KX632572.1
H1N3
T. harzianum. MG873465.1
K1N6
F2N1
T. orientale.JQ685884.1
T. longibrachiatum.AB568475.1
60
89
67
99
72
98
72
73
89
88
100
68
0.02
Section: Trichoderma
Clade: XII Rufa
Section: Pachybasium
Clade: Lixi - Catoptron
Section: Longibrachiatum

Fig. 2. Phylogenetic tree based on the sequencing results. The phylogenetic trees were drawn using MEGA 5.2 and the maximum likelihood method based on Kimura-2 parameters with 1000 bootstrap replications. *Trichoderma* species are classified as 5 sections. (a) Phylogenetic tree based on the ITS sequencing results for the 10 isolated species from this study and including 10 reference sequences obtained from GenBank that are marked with accession number next to the species name. *T. harzianum* complex belongs to the section *Pachybasium,* clade *Lixi – Catoptron*. *T. orientale, T. reesei* and *T. longibrachiatum* are classified as section *Longibrachiatum*. *T. koningii* aggregate is placed in section *Trichoderma,* clade *XII Rufa* [10, 11]. (b) and (c) are phylogenetic trees based on the *tef-1* sequencing results and *rpb-2* sequencing results, respectively, for the 10 isolated species from this study and including 10 sequences obtained from GenBank that are marked with accession number next to the species name.

hach et al. [22] declared that for the identification of *Trichoderma* species within the *T. harzianum* complex, the *tef-1* sequencing is more useful than the ITS sequencing due to some incorrect ITS sequences in the database. Fanelli et al. [23] also reclassified an isolate of *T. harzianum* (ITEM 908) as *T. atrobrunneum* split up from the *T. harzianum* complex by combination of ITS and *tef-1* sequencing. Given this close phylogenetic and morphological relatedness, an unambiguous classification is difficult, but we suggest H1N3 to be a *T. atrobrunneum* representative based on the *tef-1* and *rpb-2* results.

The high cellulolytic and glucose-tolerant isolate, H1N44 identified as *Trichoderma koningiopsis*. The morphological features of H1N44 were included fast growing rate which filled the entire Petri plates during 4 days. The color of the colony was dark green and the reverse color was colorless. Conidiophore characters included long conidiophores due to long distance between branches, opposing branches creating pyramidal structure, moderately to highly branching and curved terminal branches. Phialid shape was cylindrical to lageniform and conidia features were from subglobose to ellipsoid with green to dark green in color.

Enzyme assays. One of the limitations of *T. reesei* is its low BGL activity [5]. It is also inhibited by Glu due to the competition of substrate and Glu for the active site of the enzyme [24]. Applying exogenous BGL has been used as a solution for this problem. Therefore, isolation of *Trichoderma* strain with high BGL activity can help to design more efficient enzyme cocktails for the degradation of plant biomass [2].

Measuring the total cellulase activity (FPA assay) revealed no significant difference between the isolate H1N44 (0.66 U/mL) and *T. reesei* QM6a (0.64 U/mL) used as control (Fig. 3). However, the BGL assay showed that there was a significant difference in activity in the absence of Glu (about 4x higher) as well as Glu tolerance up to 0.6 M of Glu. In addition, evaluation of BGL activity at different temperature and pH levels showed that H1N44 had better enzyme activity than *T. reesei* at high temperatures and acidic pH (Fig. 4). Finally, evaluation revealed that H1N44 released about 3-fold more of secreted protein than *T. reesei* (3.31 vs. 1.09 mg/mL) (Fig. 5). These results showed the isolate H1N44 is promising strain in cellulase activity. The amount of total cellulase activity is almost equal in both strains. Some studies have also been done on *T. reesei* strains which consistent with FPA assay and BGL activity data in H1N44 which was identified as *T. koningiopsis*. For example, the results of FPA assay showed 0.37 and 0.72 U/mL in *T. reesei* QM9414 as original strain and an enhanced cellulase mutant, *T. reesei* RP698, respectively, after 3 days culturing on Avicel as a sole carbone source [25]. Zheng et al. [26] also compared the cellulases

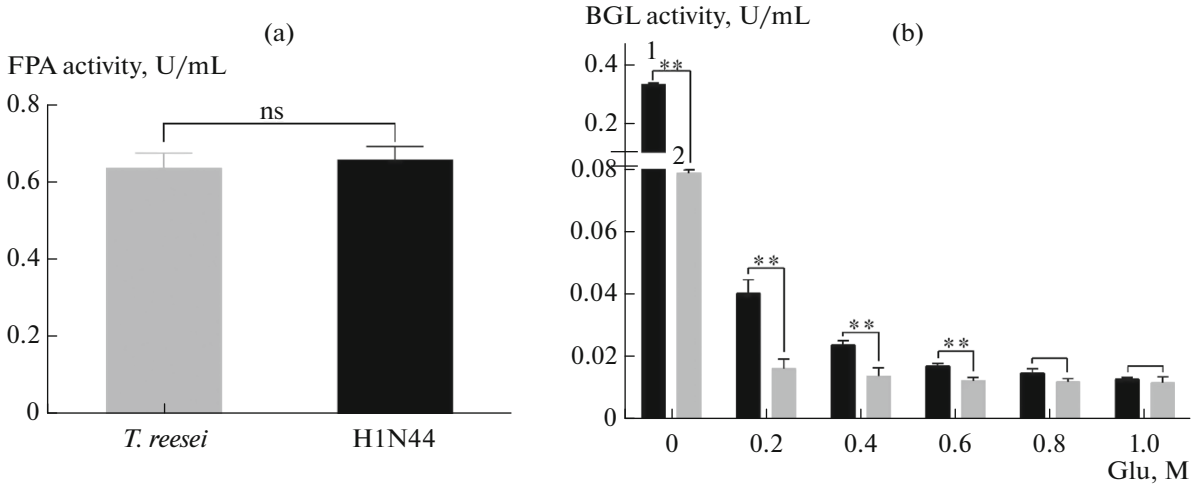

Fig. 3. Total cellulase assay (FPA activity) in *T. reesei* (QM6a) and isolate H1N44 (a), BGL activity (b) at different Glu concentrations in H1N44 (1) and *T. reesei* QM6a (2). Vertical bars indicate the standard deviation of independent triplicates: ns: $P > 0.05$, *: $P \geq 0.05$, **: $P \geq 0.01$.

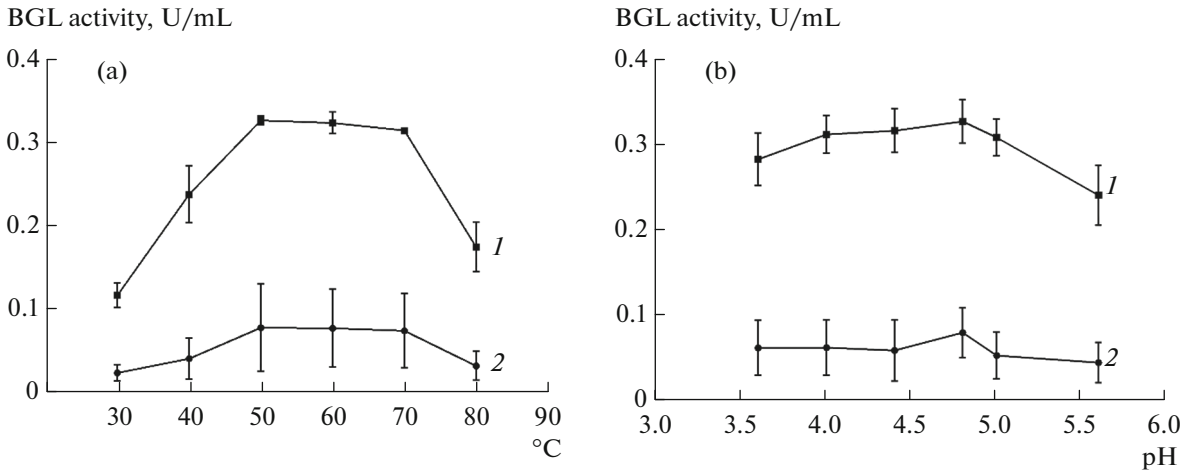

Fig. 4. Temperature (a) and pH (b) profiles of H1N44 (*1*) and *T. reesei* QM6a (*2*). Vertical bars indicate the standard deviation of independent triplicates.

activity of 3 independent Δ*Trgal11* mutants originated from *T. reesei* QM9414. The amount of total cellulase in FPA assay for the parental strain was about 0.8 U/mL and BGL activity was about 0.2 U/mL which is less than the BGL activity in H1N44 with 0.33 U/mL. An experiment performed by Peterson and Nevalaine [27] indicated that BGL activity in QM6a and *T. reesei* RUTC30 cultivated on 6% (wt/vol) roll-milled cotton was 0.3 U/mL after 14 days. BGL activity in a hyper-cellulolytic mutant *T. reesei* SS-II and its parental strain NG14 (also RUTC30) was less than 0.3 U/mL (almost equal to BGL activity in H1N44) after 6 days. The FPA was also about 0.9 U/mL in NG14 [28].

Isolation of *bgl2* gene encoding BGLII enzyme. The *bgl2* gene of the isolate H1N44 was sequenced (in partial) in order to find a possible reason for the high observed activity of BGL of the isolate H1N44 compared with *T. reesei*. Sequence comparison revealed that only Val was replaced with Cys in position 321 while the remaining important amino acids were not different (Fig. 6). A comparison of the position of this amino acid between several *Trichoderma* species revealed that this substitution also occurred in two species of *T. virens* and *T. asperellum* (Fig. 7). There are 7 amino acid residues in the active site of BGLII which are different from each other and have an effect on entrance pattern of the BGLII active site tunnel [6, 29]. Substitution of these residues effected on their kinetic parameters as well as Glu sensitivity, pH and thermostability. The outer of the active site channel includes 2 regions. One region is specified for binding to a substrate and the other one includes residues comprised the wide cleft at the entrance region of the tunnel. It is shown that changes in the amino acids at the entrance of the active site tunnel increase more activity than the substrate binding region. V321 is one of these 7 important amino acid in this region [6]. There are some studies indicated that an amino acid substitution in *bgl2* gene encoding BGL II could affect its activity. A cellulase hyper-producing mutant, *T. reesei* PC-3-7 showed increasing in cellulase production when inducer is cellobiose. A single-nucleotide mutation within the *bgl2* gene was identified by comparative genomics with its parents leading to an amino acid substitution in V409. It is concluded that this substitution could be the reason for increasing in cellulase expression when growing on cellulose and cellobiose. Lee and coworkers [6] investigated the role of amino acids in the substrate entrance region by creating mutations in the outer channel of the enzyme active site. The results exhibited 5.3- and 6.9-fold enhancement in k_{cat}/K_m and k_{cat} values in mutants P172L and P172L/F250A compared to the wild type, respectively. Guo et al. [29] improved the activity of BGLII using site-directed mutagenesis of only two

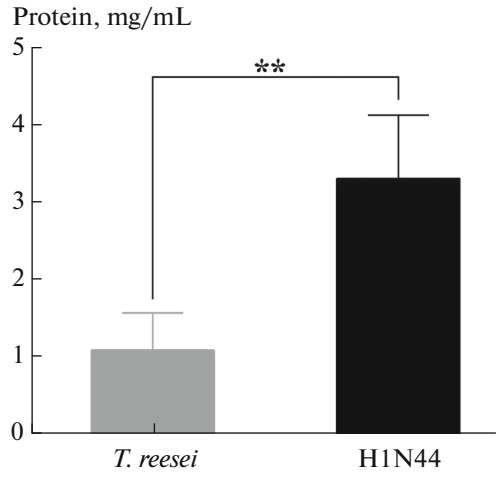

Fig. 5. Evaluation of secretory protein by Bradford method for H1N44 and *T. reesei* QM6a. Vertical bars indicate the standard deviation of independent triplicates. *$P \geq 0.05$.

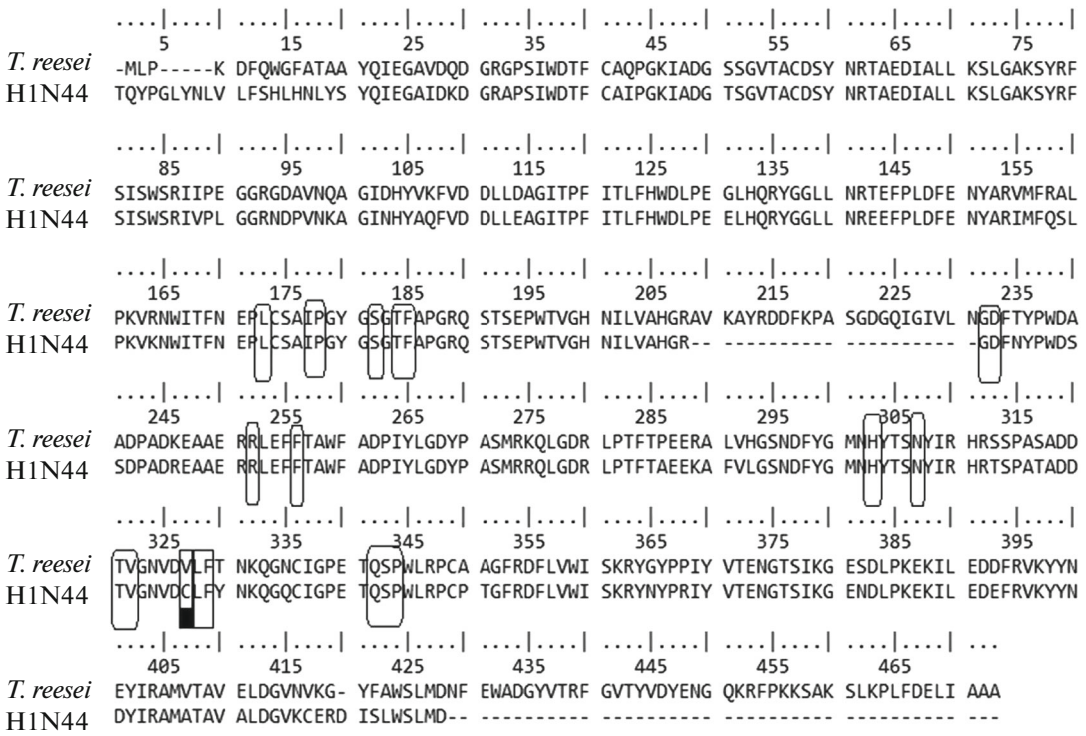

Fig. 6. Partial amino acid sequence of of the BGLII in H1N44 isolate and *T. reesei* QM6a. Rectangles represent the location of important amino acids in the active site entrance. Black square represents the only difference between the amino acids of active site entrance in position 321.

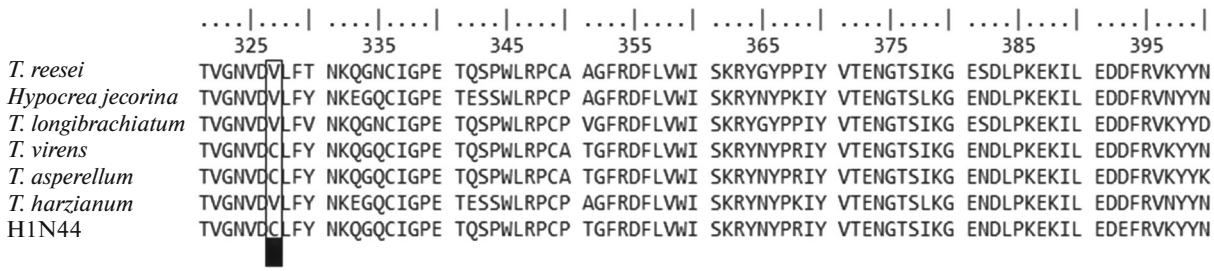

Fig. 7. A multiple sequence alignment of BGL2 *Trichoderma* sp. The protein sequences obtained from NCBI database. Black square represents the substitution of Cys and Val in the two species *T. virens* and *T. asperellum*.

amino acid residues (L167W or P172L) at the entrance of the active site. According to these studies, it can be implied that the substitution of V321C in *bgl2* gene encoding BGLII enzyme can effect on total BGL activity in our isolate H1N44 which was identified as *T. koningiopsis*. Another possibility to explain its BGL activity could be caused by presence of BGLI.

BGL enzymes in *T. reesei* were placed in 2 groups of glycosyl hydrolase families, 1 and 3. *bgl2* gene belongs to GH family 1 while *bgl1* gene was placed in GH family 3 [30]. So far, 11 extracellular and intracellular BGLs have been identified in *T. reesei*. One of the most important extracellular β-glucosidases is BGL1 [30]. BGLII is also an important enzyme in induction of cellulase and conversion of cellobiose to sophorose which is an efficient cellulase inducer. Some studies concluded that the BGLII is likely an intracellular BGL and not a secreted protein in *Trichoderma* [31]. It is discussed by Zhou et al. [32] that a rapid induction of cellulase genes was occurred by BGLII on cellulose and cellobiose based on the physiological role of BGLII. It can form a glycosidic linkage by reverse hydrolysis between 2 Glus which bind to its active site at high Glu concentration [33]. According to this point that the BGLII is an intracellular enzyme, total activity of BGL could be related to BGLI enzyme not the BGLII. In addition, the result of Zhang et al. [34] suggested that high BGL activity of *T. koningiopsis* was due to the high concentration of BGL belonging to family 3 which includes BGLI.

As it mentioned above, there are 11 genes encode BGLs. The reason for presence of this number of genes in *T. reesei* genome as well as the role of each BGL in cellulase production is unclear. BGLs in *T. reesei* were classified in 4 groups based on their patterns of the cellular distribution including; 1) vesicles for protein secretion in the cytoplasm, 2) similar to a reticular network via forming the whole endomembrane and cell membrane with protein aggregation, 3) in vacuoles and, 4) in the nucleus [35]. In contrast with the previous studies which suggested that the BGLII is intracellular, Pang and coworkers [35] believed that the BGLII is an extracellular enzyme. BGLII does not secreted by conventional secretion protein pathway due to containing no signal peptide. It was instead secreted via vacuole-mediated secretory pathway which vacuoles were fused to the lateral plasma membrane and proteins were secreted from them. According to these findings, it can be argued that both BGLI and BGLII are involved in total BGL activity.

The study of the *bgl2* sequence in the best isolate (H1N44) revealed that a substitution among the amino acids in the entrance region of the active site might be involved in Glu tolerance. This substitution has also occurred in *T. virens* and *T. asperellum*. Although no significant report could be found for BGL activity and Glu tolerance of these two species, we hypothesize that this substitution can affect the enzyme activity in H1N44 compared with *T. reesei* QM6a. Secretion of protein was also 3-fold higher in the H1N44 than in *T. reesei* QM6a. Glu tolerance in H1N44 might, thus, also benefit from the high concentration of cellulase enzyme.

* *

In conclusion, we isolated 77 *Trichoderma* strains from forest soils in Iran. Out of these, 10 cellulolytic isolates were identified. For final clarification and in some ambiguous cases, a combination of several methods including the sequencing of at least 3 genetic loci is nevertheless necessary. In the following, the isolates were qualitatively screened for selection of the best cellulolytic and Glu-tolerant isolate, leading to the identification of H1N44 as the best isolate, which exhibited high total cellulase and BGL activity. According to these results, the cellulolytic isolate H1N44 with high BGL activity and low Glu inhibition can be considered as a promising strain for follow-up studies with industrial approaches.

ACKNOWLEDGMENTS

The authors would like to express special thanks to Prof. Dr. P. Benz (Technische Universität München, Germany) for his help with sequencing and critical reading of the manuscript. Furthermore, we would like to thank S. Klasen (Technische Universität München, Germany) for her help in sequencing.

FUNDING

This work was funded by the Ferdowsi University of Mashhad, Iran (Grant no.: 3/43048) and Iran National Science Foundation (INSF) (Grant no.: 95849817).

COMPLIANCE WITH ETHICAL STANDARDS

The authors declare that they have no conflicts of interest. This article does not contain any studies involving animals or human participants performed by any of the authors.

DATA AVAILABILITY

All datasets are presented in the manuscript. The sequences generated in this study are submitted in NCBI Bank (https://www.ncbi.nlm.nih.gov).

REFERENCES

1. Fujii. T., Inoue, H., and Ishikawa, K., *AMB Express*, 2013, vol. 3, no. 1, pp. 1–9. https://doi.org/10.1186/2191-0855-3-73
2. Singhania, R.R., Patel, A.K., Sukumaran, R.K., Larroche, C., and Pandey, A., *Bioresour. Technol.*, 2012, vol. 127, pp. 500–507. https://doi.org/10.1016/j.biortech.2012.09.012
3. Singhania, R.R., Sukumaran, R.K., Patel, A.K., Larroche, C., and Pandey, A., *Enzyme Microbiol. Technol.*, 2010, vol. 46, no. 7, pp. 541–549. https://doi.org/10.1016/j.enzmictec.2010.03.010
4. Wen, Z., Liao, W., and Chen, S., *Process Biochem.*, 2005, vol. 40, no. 9, pp. 3087–3094. https://doi.org/10.1016/j.fensle.2005.08.034
5. Rahman, Z., Shida, Y., Furukawa, T., *Biosci. Biotechnol. Biochem.*, 2009, vol. 73, no. 5, pp. 1083–9. https://doi.org/10.1271/bbb.80852
6. Lee, H.L., Chang, C.K., Jeng, W.Y., Wang, A.H., and Liang, P.H., *Protein Eng., Des. Sel.*, 2012, vol. 25, no. 11, pp. 733–740. https://doi.org/10.1093/protein/gzs073
7. Salgado, J.C.S., Meleiro, L.P., Carli, S., and Ward, R.J., *Bioresour. Technol.*, 2018, vol. *267*, no. 2018, pp. 704–713.
8. Zhang, C.L., Druzhinina, I.S, Kubicek, C.P., and Xu, T., *FEMS Microbiol. Lett.*, 2005, vol. 251, no. 2, pp. 251–257. https://doi.org/10.1016/j.femsle.2005.08.034.z
9. *Trichoderma and Gliocladium: Basic Biology, Taxonomy and Genetics*, Kubicek C.P., and Harman, G.E., Eds., London: Taylor and Francis, 1998, vol. 1, pp. 3–34. https://doi.org/10.1201/9781482295320
10. Druzhinina, I. and Kubicek, C.P., *J. Zhejiang Univ., Sci., B.*, 2005, vol. 6, no. 2, pp. 100–112. https://doi.org//10.1631/jzus.2005.B0100
11. Druzhinina, I.S., Kopchinskiy, A.G., Komoń, M., Bissett, J., Szakacs, G., and Kubicek, C.P., *Fungal*

Genet. Biol., 2005, vol. 42, no. 10, pp. 813–828. https://doi.org/10.1016/j.fgb.2005.06.007

12. *The Dynamical Processes of Biodiversity—Case Studies of Evolution and Spatial Distribution,* Grillo, O. and Venora, G., Eds., Intech., 2011, pp. 303–320.
13. Florencio, C., Couri, S., and Farinas, C.S., *Enzyme Res.*, 2012, vol. 2012. https://doi.org/10.1155/2012/793708
14. Doyle, J., *Molecular Techniques in Taxonomy*, Hewitt, G.M., Johnston, A.W.B., and Young, J.P.W., Eds., Berlin: Springer, 1991, vol. 57, pp. 283–293.
15. Mandels, M. and Weber, J., *Cellulases and Their Applications*, Hajny, G.J. and Reese, E.T., Eds., Washington, DC: Advances in Chemistry; American Chemical Society, 1969, vol. 95, chapter 23, pp. 391–414.
16. Ghose, T.K., *Pure Appl. Chem.*, 1987, vol. 59, no. 2, pp. 257–268. https://doi.org/10.1351/pac198759020257
17. Zhang, Y.H.P., Hong, J., and Ye,X., *Biofuels: Methods and Protocols,* Mielenz J.R., Eds., Methods Mol. Biol., New York: Humana, 2009, vol. 581, chapter 14, pp. 213–231.
18. Bradford, M.M., *Anal. Biochem.,* 1976, vol. 72, nos. 1–2, pp. 248–254.
19. Chuster, A. and Schmoll, M., *Appl. Microbiol. Biotechnol.*, 2010, vol. 87, no. 3, pp. 787–799. https://doi.org/10.1007/s00253-010-2632-1
20. Samuels, G.J., Petrini, O., Kuhls, K., Lieckfeldt, E., and Kubicek, C.P., *Stud. Mycol.*, 1998, vol. 41, pp. 1–54.
21. Chaverri, P., Branco-Rocha, F., Jaklitsch, W., Gazis, R., Degenkolb, T., and Samuels, G.J., *Mycologia*, 2015, vol. 107, no. 3, pp. 558–590. https://doi.org/10.3852/14-147
22. Haouhach, S., Karkachi, N., Oguiba, B., Sidaoui, A., Chamorro, I., Kihal, M., et al., *Microorganisms.*, 2020, vol. 8, no. 10, pp. 1455–1469. https://doi.org/10.3390/microorganisms8101455
23. Fanelli, F., Liuzzi, V.C., Logrieco, A.F., and Altomare, C., *BMC Genomics*, 2018, vol. 19, no. 1, pp. 1–18. https://doi.org/10.1186/s12864-018-5049-3
24. Teugjas, H. and Väljamäe, P., *Biotechnol. Biofuels*, 2013, vol. 6, no. 1, pp. 1–3. https://doi.org/10.1186/1754-6834-6-105
25. Silva, J.C.R., Salgado, J.C.S., Vici, A.C., Ward, R.J., Polizeli, M.L.T.M., Guimarães, L.H.S., et al., *Braz. J. Microbiol.*, 2020, vol. 51, no. 2, pp. 537–545. https://doi.org/10.1007/s42770-019-00167-2
26. Zhang, Z., Liu, J.L., Lan, J.Y., Duan, C.J., Ma, Q.S., and Feng, J.X., *Biotechnol. Biofuels*, 2014, vol. 7, no. 1, pp. 1–14. https://doi.org/10.1186/1754-6834-7-107
27. Peterson, R. and Nevalainen, H., *Microbiology*, 2012, vol. 158, no. 1, pp. 58–68. https://doi.org/10.1099/mic.0.054031-0
28. Liu, P., Lin, A., Zhang, G., Zhang, J., Chen, Y., Shen, et al., *Microb. Cell Fact.,* 2019, vol. 18, no. 1, pp. 1–16. https://doi.org/10.1186/s12934-019-1131-z
29. Guo, B., Amano, Y., and Nozaki, K., *PLoS One*, 2016, vol. 11, no. 1. https://doi.org/10.1371/journal.pone.0147301
30. Zou, G., Jiang, Y., Liu, R., Zhu, Z., and Zhou, Z., *Biotechnol Biofuels*, 2018, vol. 11, no. 314. https://doi.org/10.1186/s13068-018-1314-6
31. Saloheimo, M., Ylösmäki, E., Ward, M., and Penttilä, M., *Appl. Environ. Microbiol.*, 2002, vol. 68, no. 9, pp. 4546–4553. https://doi.org/10.1128/AEM.68.9.4546-4553.2002
32. Zhou, Q., Xu, J., Kou, Y., Lv, X., Zhang, X., Zhao, G., et al., *Eukaryot. Cell*, 2012, vol. 11, no. 11, pp. 1371–1381. https://doi.org/10.1128/EC.00170-12
33. Mackenzie, L.F., Wang, Q., Warren, R.A.J., and Withers, S.G., *J. Am. Chem. Soc.*, 1998, vol. 120, pp. 5583–5584.
34. Zhang, Z., Liu, J.L., Lan, J.Y., Duan, C.J., Ma, Q.S. and Feng, J.X., *Biotechnol. Biofuels*, 2014, vol. 7, no. 107, pp. 1–14. https://doi.org/10.1186/1754-6834-7-107
35. Pang, A.P., Wang, H., Luo, Y., Yang, Z., Liu, Z., Wang, Z., et al., *mBio.*, 2021, vol. 12, no. 3, pp. e03671-20. https://doi.org/10.1128/mBio.03671-20